Title
Measurements of the eigenfunction of reversed shear Alfvén eigenmodes that sweep downward in frequency

Journal
Physics of Plasmas, 20(8)

ISSN
1070-664X

Authors
Heidbrink, WW
Austin, ME
Spong, DA
et al.

Publication Date
2013-08-01

DOI
10.1063/1.4817950

Measurements of the eigenfunction of reversed shear Alfvén eigenmodes that sweep downward in frequency

W. W. Heidbrink,[1,a)] M. E. Austin,[2] D. A. Spong,[3] B. J. Tobias,[4] and M. A. Van Zeeland[5]
[1]*University of California Irvine, Irvine, California 92697, USA*
[2]*University of Texas at Austin, Austin, Texas 78712, USA*
[3]*Oak Ridge National Laboratory, Oak Ridge, Tennessee 37831, USA*
[4]*Princeton Plasma Physics Laboratory, Princeton, New Jersey 08543, USA*
[5]*General Atomics, San Diego, California 92186, USA*

(Received 6 June 2013; accepted 23 July 2013; published online 9 August 2013)

Reversed shear Alfvén eigenmodes (RSAEs) usually sweep upward in frequency when the minimum value of the safety factor q_{min} decreases in time. On rare occasions, RSAEs sweep downward prior to the upward sweep. Electron cyclotron emission measurements show that the radial eigenfunction during the downsweeping phase is similar to the eigenfunction of normal, upsweeping RSAEs. © *2013 AIP Publishing LLC*. [http://dx.doi.org/10.1063/1.4817950]

I. INTRODUCTION

Reversed shear Alfvén eigenmodes (RSAE) are instabilities that are driven unstable by energetic ion populations in tokamak plasmas with an off-axis minimum in the safety factor q_{min}.[1–3] RSAEs cause fast-ion transport.[4–7] They also provide accurate information about the evolution of the q profile: When q_{min} is an integer value, a "grand cascade" of many RSAEs with different toroidal mode numbers n is often observed.[2]

In the laboratory frame, the frequency ω of an RSAE is approximately[8]

$$\omega = \left[\left(\frac{m}{q_{min}} - n\right)^2 \frac{v_A^2}{R_0^2} + \omega_{GAM}^2\right]^{1/2} + \delta\omega + n\omega_{rot}, \qquad (1)$$

where m is the poloidal mode number, v_A is the Alfvén speed, R_0 is the major radius, the frequency of geodesic acoustic modes (GAMs) or beta-induced Alfvén eigenmodes (BAEs) is

$$\omega_{GAM}^2 = \frac{2}{m_i R_0^2}\left(T_e + \frac{7}{4}T_i\right), \qquad (2)$$

$\delta\omega$ is an additional frequency shift associated with pressure effects, and $n\omega_{rot}$ is the Doppler shift associated with toroidal rotation of the plasma. Here, m_i is the ion mass, and T_e and T_i are the electron and ion temperature. The mode frequency [Eq. (1)] is smallest when q_{min} is the rational number $q_{min} = m/n$. In normal tokamak operation, q_{min} decreases in time as the plasma current diffuses toward the magnetic axis. In the vast majority of published cases,[1–5,8–21] the modes first appear when $q_{min} = m/n$, then the mode frequency sweeps upward in frequency as the q profile evolves. Very rarely,[8,22,23] a mode will sweep downward to the minimum frequency, then sweep upward in the normal fashion. In a Joint European Torus (JET) database, this phenomenon was observed "in only 26 discharges as opposed to more than 5000 discharges where upward sweeping" RSAEs were observed.[23] [Note that downward sweeps are often observed for RSAEs that have transformed into a toroidal Alfvén eigenmode (TAE) at the maximum of the frequency sweep. See, for example, Fig. 10 in Ref. 24. This is a different phenomenon that is readily understood by conventional TAE theory.]

Published work on the RSAE eigenfunction has focused on normal upsweeping RSAEs. Reflectometry measurements have shown that the eigenfunction peaks near the q_{min} radius and that the density fluctuation is largest at small major radius R.[11,16] Coherence profiles from reflectometry (a measure of signal-to-noise) are similar during the downsweeping and upsweeping phases.[25] Electron cyclotron emission (ECE) measurements of the electron temperature fluctuation have shown that the radial mode structure agrees approximately with ideal MHD predictions.[13] The first two radial harmonics predicted by MHD theory have been observed.[26] Near the minimum frequency, the poloidal structure is dominated by a single poloidal harmonic[26,27] that transforms into a structure dominated by two poloidal harmonics as the frequency approaches the TAE frequency.[28] Although ideal MHD theory predicts constant phase across the eigenfunction, measurements show that the phase changes with radius.[27,29]

In recent years, numerous theories have been proposed to explain why downsweeping RSAEs are rare. One theory[23,30,31] argues that the potential well that allows formation of the RSAE during the upsweeping phase is a potential hill during the downsweeping phase, so the downsweeping instabilities are actually quasimodes.[30,31] Observations of downsweeping RSAEs during radio-frequency (RF) heating in JET support this interpretation.[23] Another possibility is that the downsweeping modes are a kinetic RSAE (KRSAE) made possible by finite Larmor radius (FLR) effects.[32] This occurs when the ratio of fast-ion gradient to second derivative of the q profile q''_{min} is relatively small. A paper by Yu *et al.*[33] shows that the KRSAE eigenfunction is often modulated radially on the ion Larmor radius scale. Marchenko and Reznik[34] suggest that downsweeping RSAEs are actually

a)Electronic mail: heidbrink@fusion.gat.com

infernal modes that occur when the q profile is very flat in the core. They state that eigenfunction measurements could distinguish between a quasimode with mode structure localized around q_{min} and an infernal mode with a mode structure that occupies the whole low-shear core. Gorelenkov *et al.*[35] analyze RSAEs analytically and numerically, finding that: "Even though experiments show that the down sweep instability continuously transforms to the sweep bottom and to the up sweeping case, their radial structures are different." Their study suggests that the criteria for mode existence are more stringent for downsweeping instabilities than for upsweeping modes. Haverkort[36] considers the effects of toroidal rotation on RSAE existence criteria. He argues that downsweeping can occur when q_{min} has a local maximum or when the toroidal mode number n is high and the rotation frequency is locally concave.

The purpose of this paper is to present radial eigenfunction data that may discriminate between these theoretical explanations. Measurements of the eigenfunctions of downward sweeping RSAEs are presented in Sec. II. Section III discusses the theoretical implications of the measurements. The conclusions are in Sec. IV.

II. EXPERIMENT

The discharges for this study are from dedicated experiments of Alfvén eigenmodes on the DIII-D tokamak between 2005 and 2012. To insure availability of ECE data, all discharges have toroidal fields of approximately 2 T. The plasma is deuterium and the primary impurity is carbon from the graphite walls (typically $Z_{eff} \simeq 1.5$). The energetic ion population is produced by deuterium neutral-beam injection of neutrals with energies ≤ 81 keV. The angles of beam injection include on-axis and off-axis, co-current and counter-current, and near-tangential and near-perpendicular. The neutral beams inject during the current ramp and drive RSAE and TAE activity. Most discharges are limited on the inside wall, have relatively low density ($\sim 2.5 \times 10^{13}$ cm^{-3}), and are L-mode plasmas. Plasma shapes include circular, oval, and D-shaped plasmas. Electron cyclotron heating at radii both inside and outside q_{min} is applied in some of the discharges.

EFIT[37] equilibrium reconstructions utilize magnetic and motional Stark effect[38] data, as well as the times of integer and half-integer q_{min} crossings inferred from the Alfvén "cascade" behavior,[2] allowing determination of q_{min} to an accuracy of ± 0.1.

The cross-power of signals from two CO_2 interferometer chords provides a basic monitor of Alfvén eigenmode activity.[39] A typical discharge has dozens of upsweeping RSAEs. A survey of interferometer spectrograms from >150 discharges reveals only a handful of clear examples of downsweeping RSAEs. A complication in identification of downsweeping modes is that, if the mode amplitude is weak, the mode may appear and disappear; when it reappears at slightly different frequency, it is difficult to determine if it is the same mode or, for example, a different radial harmonic with slightly different frequency. Despite these experimental difficulties, it is unquestionably true that downsweeping is rare, occurring on the order of 0.1% of the cases. This frequency of occurrence is similar to the one reported for JET discharges.[23]

Two types of downsweeping RSAEs are observed. Figure 1(a) shows an example of "fishhook" behavior. At ~460 ms, a mode appears that sweeps down ~5 kHz in frequency prior to the normal, upsweeping phase. Figure 1(b) shows an example of the second type of downsweeping RSAE. In this discharge, $q_{min} = 4$ at ~525 ms. A few modes sweep down to the frequency minimum; at the minimum, many modes appear; after the minimum, a few RSAEs sweep upward in frequency in the normal fashion. These phenomena sometimes occur at an integer q_{min} crossing and appear as "fuzz" at the minimum frequency on the interferometer cross-power spectra.

Eigenfunction information is provided by an ECE radiometer that measures electron temperature fluctuations $\tilde{T}_e$ on a radial chord near the midplane,[40] an ECE imaging diagnostic that measures $\tilde{T}_e$ in two rectangular regions,[41] and a beam emission spectroscopy (BES) diagnostic that measures electron density fluctuations $\tilde{n}_e$ at 64 variable locations.[42] Toroidal mode numbers are inferred from a toroidal array of magnetic coils and from the Doppler shift and temporal evolution of upsweeping RSAEs.

Sequences of fast Fourier transforms (FFTs) of ECE radiometer data diagnose possible changes in mode structure during the frequency sweep. The parameters for the FFTs are 1024 points, 50% overlap of time windows, 1 kHz frequency smoothing, and Hanning filtering of the time series data. Figure 2 shows a sequence of FFTs vs major radius for a normal, upsweeping RSAE. The mode first

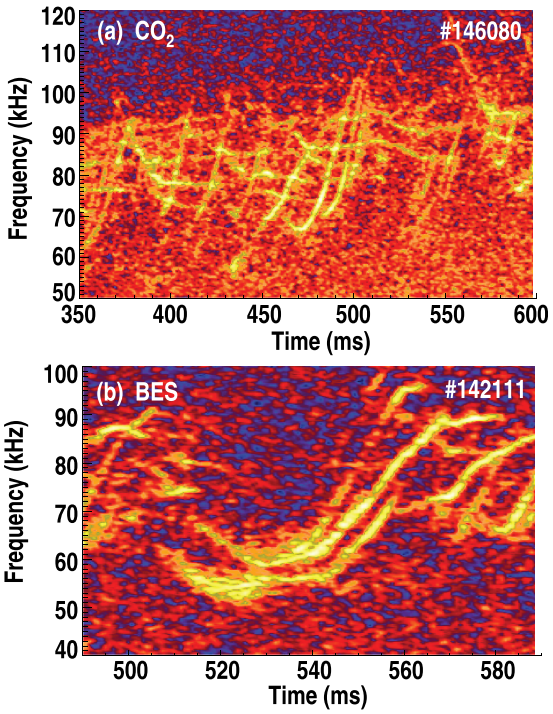

FIG. 1. (a) Cross-power of two CO_2 interferometer signals. A downsweeping RSAE occurs at 470 ms. (b) Cross-power of two BES signals. A large number of modes appear at $t \simeq 525$ ms when the downsweeping $n = 2$ and $n = 3$ modes cross $q_{min} = 4$.

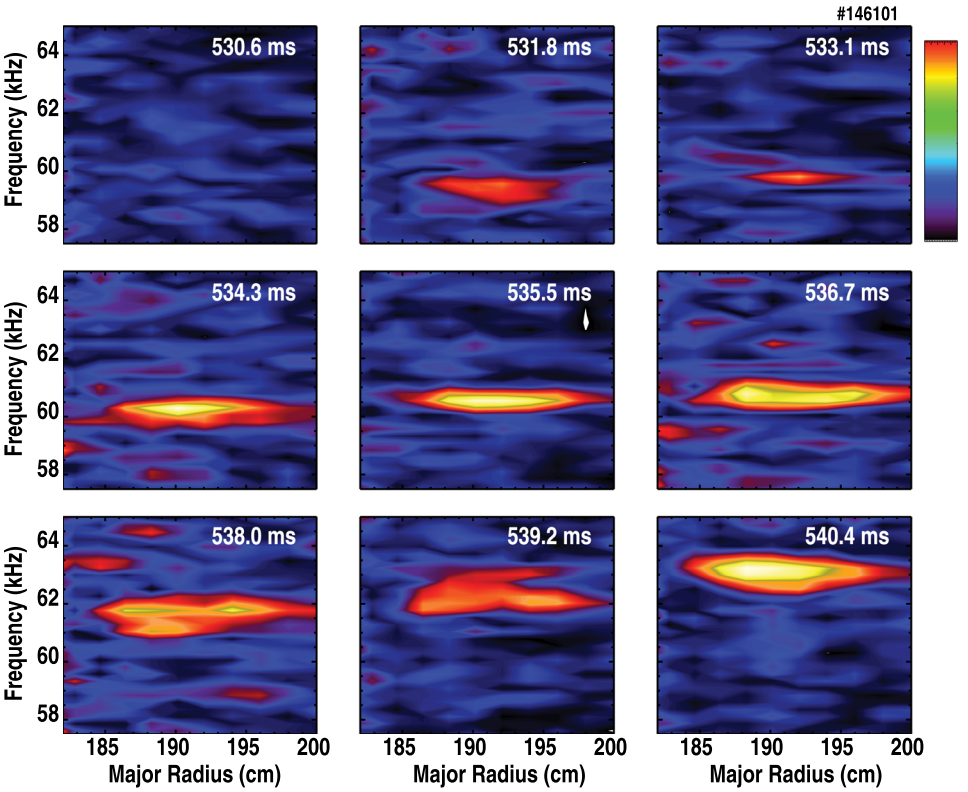

FIG. 2. Contour plot of the amplitude of $\delta T_e/T_e$ vs channel major radius and frequency for an ordinary RSAE that sweeps up from the minimum. The "rainbow" linear color scale shown in the upper righthand corner is also employed in Figs. 3 and 4.

appears at its minimum frequency (at 531.8 ms), then sweeps upward in frequency. Changes in radial mode structure as the frequency evolves are modest. This particular discharge uses off-axis neutral beam injection, which results in relatively weak RSAE drive[43] and minimizes changes in mode structure caused by coupling to other unstable modes.[44]

Figure 3 shows a similar sequence of ECE spectra for a downsweeping "fishhook" case. The mode is first visible ~5 ms before the frequency minimum at a frequency that is ~4 kHz higher than the minimum. As the mode sweeps down to the minimum then back up in frequency, changes in mode structure appear modest. This discharge also utilizes off-axis neutral beam injection to drive RSAEs weakly.

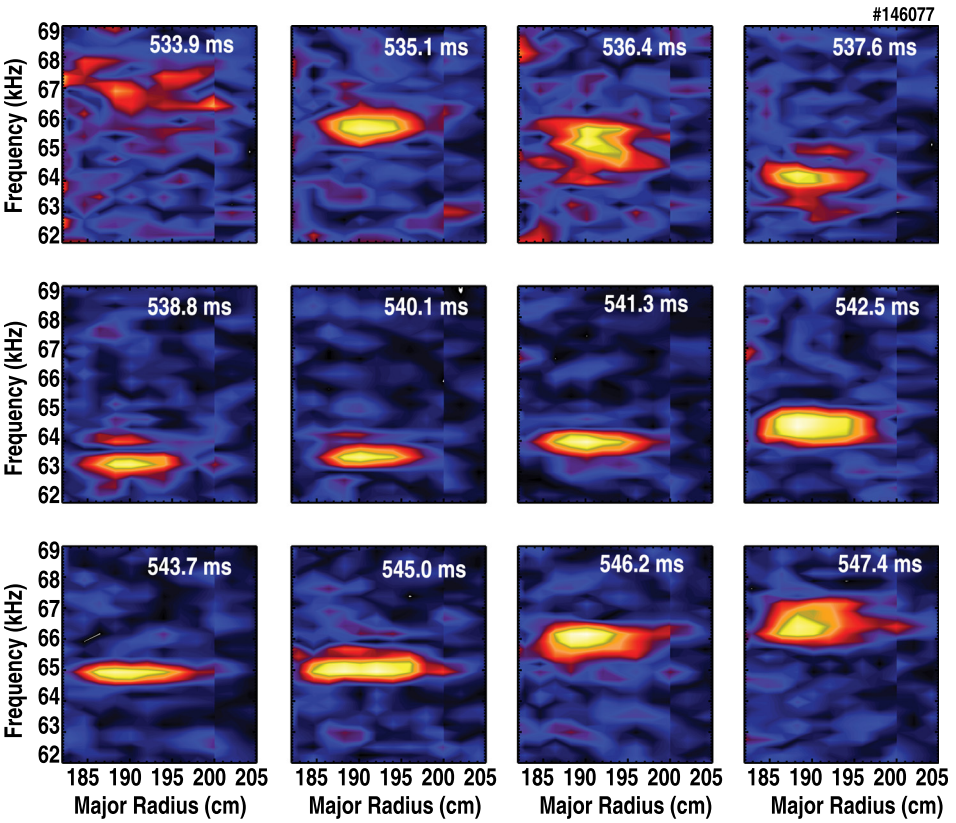

FIG. 3. Contour plot of the amplitude of $\delta T_e/T_e$ vs channel major radius and frequency for a downsweeping RSAE.

Figure 4 shows the sequence of ECE spectra for a downsweeping "fuzz" case where multiple $n=2$ modes appear when $q_{min}=4$. This case has on-axis injection and is more strongly driven. Because of the multiple modes, tracking a particular mode is challenging but it appears that the most unstable mode sweeps downward in frequency prior to the minimum. At the minimum, many bands appear. This could indicate that several modes are unstable or it could reflect amplitude modulation of the primary mode at ~1 kHz. Subsequently, a single RSAE begins its upward frequency sweep. Throughout the evolution, the modes are localized near q_{min}.

Detailed analysis of ECE cross-power spectra for a fishhook case is shown in Fig. 5. The mode occurs when $q_{min} \simeq 4.3$ and is an $n=3$ mode. Analysis of Eq. (1) near $q_{min}=m/n$ predicts a quadratic dependence of the frequency at the minimum if q_{min} falls linearly with time. Experimentally, the frequency sweeps down to the minimum with an approximately parabolic shape [Fig. 5(a)], as expected. At this time, the GAM frequency is ~39 kHz at q_{min} and the Doppler shift $nf_{rot} \simeq 12$ kHz, so $\delta\omega/(2\pi) \simeq 15$ kHz, a typical value for these DIII-D conditions. The mode amplitude is smaller before the minimum [Fig. 5(b)]. Although there is substantial variation in the channel-to-channel amplitudes as the mode evolves, the overall envelope of the mode remains invariant [Fig. 5(c)]. The phase of the mode exhibits radial shearing that shifts in slope as the mode evolves [Fig. 5(d)].

Measurements of the same mode with the ECE imaging diagnostic confirm the invariance of the mode structure. Figure 6 compares images from the downsweeping and upsweeping phases. Apart from the amplitude ($\delta T_e/T_e \simeq 0.6\%$ rms before; 0.9% after), the images are indistinguishable. In addition to the measured data (rectangular boxes), the figure shows the reconstructed poloidal structure. The reconstruction is consistent with a $(m,n)=(13,3)$ mode.

Examination of other fishhook cases shows that the trends shown in Figs. 5(a)–5(c) are generally observed. Phase variations as the mode evolves [Fig. 5(d)] are also generally observed but the shape of the curves and the sign of the slope differs for different cases.

It is unclear why fishhook behavior occurs in some cases but not in others. There is nothing unusual about the plasma parameters in the discharges with downsweeping RSAEs. Also, within a discharge with a fishhook, there is no obvious change in plasma profiles that cause the transition from ordinary RSAEs to fishhook RSAEs. Figure 7 shows plasma profiles at the time of the fishhook RSAE of Fig. 5 and at the time of the "fuzz" RSAE of Fig. 4. These are ordinary density, temperature, rotation, and q profiles for beam-heating during the current ramp in DIII-D. Admittedly, within experimental uncertainties, there may be subtle variations in profile shape near q_{min} that are not detected by the diagnostics. The available Thomson scattering measurements of electron density[45]

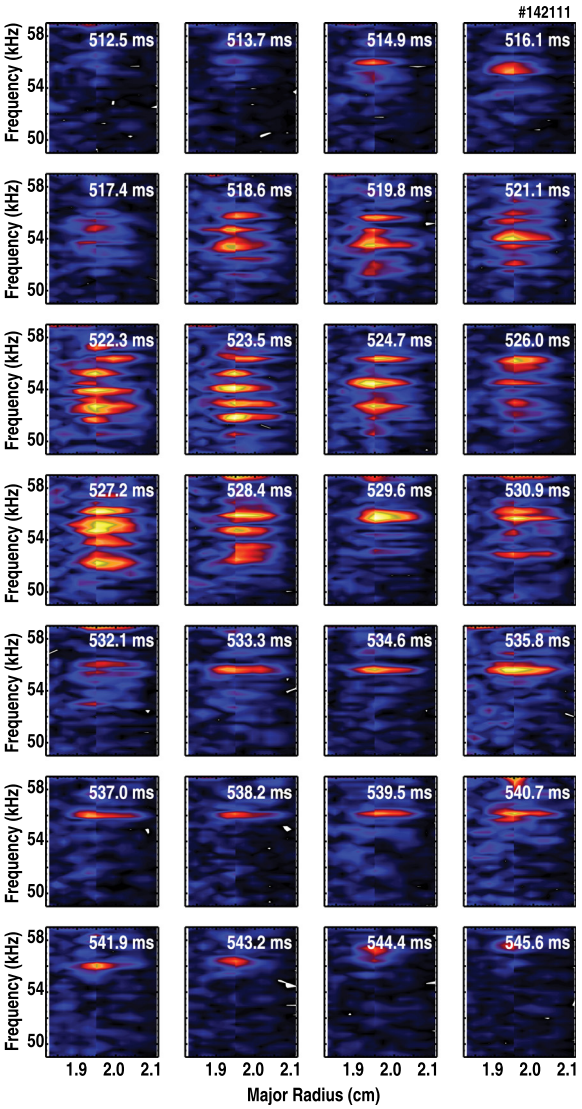

FIG. 4. Contour plot of the amplitude of $\delta T_e/T_e$ vs channel major radius and frequency for a case with many modes at the frequency minima.

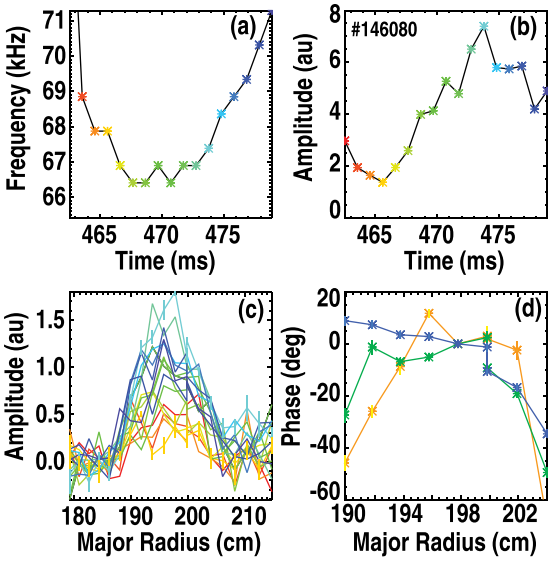

FIG. 5. (a) Frequency and (b) spatially averaged amplitude vs time for a downsweeping RSAE. The symbols on the curves indicate the time slices shown in the subsequent figures. (c) Cross-power and (d) cross-phase vs major radius at several different times. The estimated noise floor has been subtracted from the amplitude figures; the representative error bars are derived from the noise floor. The cross-phase error is $\sqrt{(1/c-1)/2}$, where c is the coherence squared.

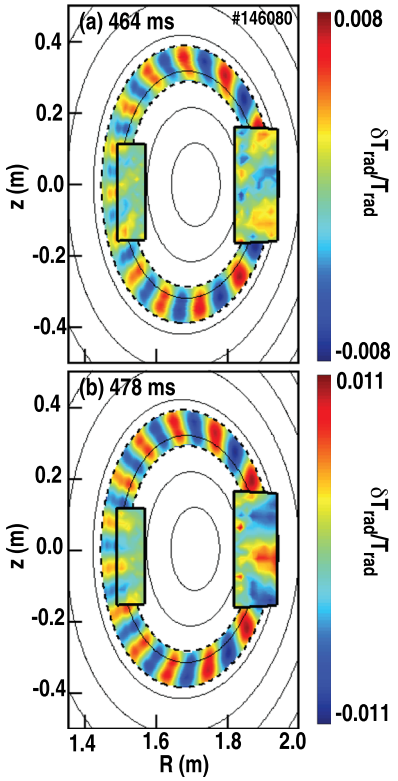

FIG. 6. ECE imaging measurements (a) 5 ms before the minimum in mode frequency and (b) 8 ms after the minimum for the same mode as in Fig. 5. The measured data on the inside and outside of the magnetic axis appear in the rectangular boxes; the poloidal reconstruction is from a fit to the data.

provide no constraints on ∇n_e near q_{min}. Approximately 50% variations in ∇T_e are consistent with the ECE electron temperature measurements. The channel-to-channel spacing of ~3 cm and ~10% errors in the charge exchange recombination spectroscopy measurements of ion temperature and toroidal rotation[46] could mask large variations in ∇T_i and ∇f_{rot}.

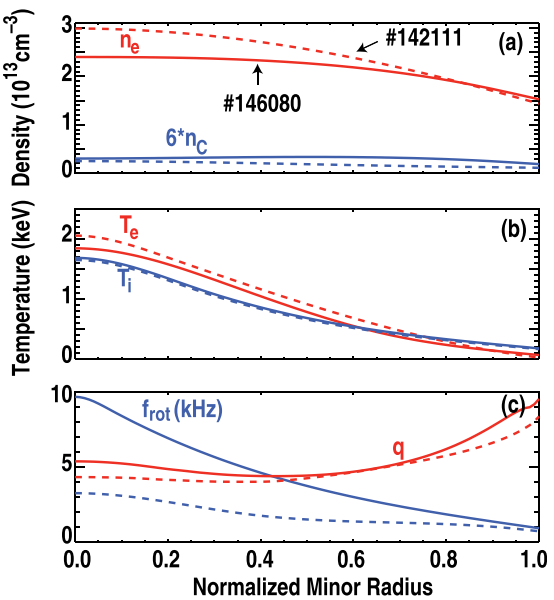

FIG. 7. Plasma profiles for the examples of Fig. 3 (solid) and 4 (dashed). (a) Electron and carbon density, (b) electron and ion temperature, and (c) Toroidal rotation frequency and safety factor.

The q profile is determined from EFIT[37] equilibrium reconstructions that use magnetics, motional Stark effect,[38] electron temperature, and RSAE behavior as constraints but, although these are relatively accurate equilibria, the value of q'' near q_{min} is poorly constrained. Also, the fast-ion D-alpha measurements of the fast-ion profile[47–49] are too inaccurate to provide meaningful constraints on the fast-ion gradient near q_{min}. To summarize, global variations in profiles cannot explain the appearance of downsweeping RSAEs but local variations may be responsible.

The examples given above are representative of the observations in discharges with predominately co-current injection. For completeness, a secondary survey of discharges with predominately counter-injection is summarized here. In rare instances, modes with long downsweeping phases are observed (Fig. 8). Unfortunately, none of these rare events have ECE data that unambiguously tracks the evolution of the eigenfunction. The few extant examples usually have lower toroidal mode numbers than the majority of DIII-D RSAEs.

III. DISCUSSION

Although rare, the observed downsweeping RSAEs seem very similar in mode structure and plasma conditions to ordinary upsweeping RSAEs. This may suggest that theories that attribute their rarity to mode existence criteria are incorrect. Experimentally, when observed, the amplitude of downsweeping RSAEs generally increases as the frequency passes through the minimum, suggesting that it is the balance between damping and drive (stability considerations) that governs their appearance.

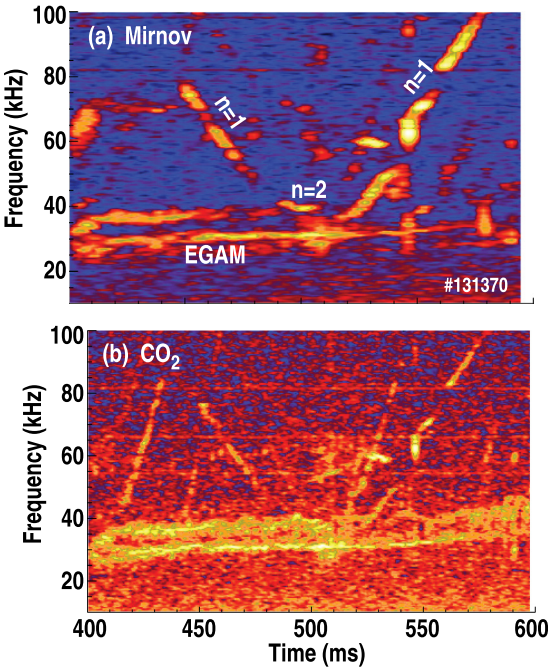

FIG. 8. Cross-power of (a) two magnetic probes and (b) two CO_2 interferometer signals in a reversed-shear plasma with 2.5 MW of counter injection, $n_e = 2.1 \times 10^{13}$ cm^{-3}, $B_T = 2.0$ T, and $I_p \simeq 0.8$ MA. The long downsweeping mode has toroidal mode number $n = 1$. The strong modes with steady frequencies at ~30 kHz are energetic particle driven geodesic acoustic modes (EGAMs).[50]

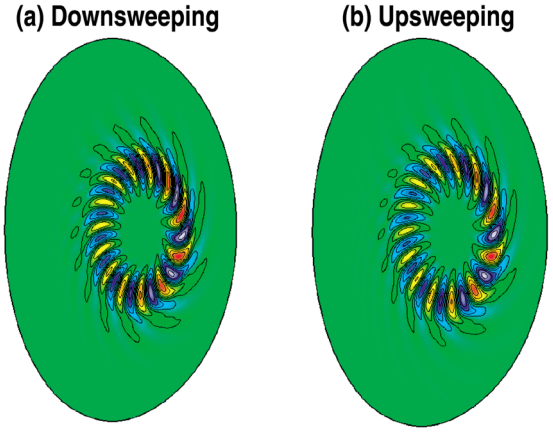

FIG. 9. TAEFL calculations of the eigenfunction of an $n = 4$ RSAE in the discharge of Fig. 4 during the (a) downsweeping and (b) upsweeping frequency phases. The frequency minimum occurs at $q_{min} = 3.25$; the downsweeping and upsweeping eigenfunctions are for $q_{min} = 3.26$ and 3.22, respectively.

The only theory that is excluded by the mode structure data is the hypothesis that downsweeping RSAEs are infernal modes.[34] Experimentally, the radial eigenfunctions of fishhook RSAEs are localized near q_{min} and do not extend throughout the plasma core.

The hypothesis that downsweeping modes are related to kinetic RSAEs[33] is harder to evaluate. The spatial resolution of the ECE radiometer is ~5 cm poloidally and ~1 cm radially, with a channel-to-channel spacing of ~2 cm. Taking into account signal-to-noise issues, it is possible that the radial amplitude modulations predicted for kinetic RSAEs are consistent with the data, although there is no compelling evidence that the mode structure is different during the downsweeping phase. Thus, there is no experimental support for the prediction of Gorelenkov *et al.*[35] that downsweeping RSAEs have different radial structures.

Recently, upsweeping DIII-D RSAEs were modeled by the gyrofluid TAEFL code[27,28] and by the gyrokinetic GTC,[51] GYRO,[52] and GEM[53] codes. The calculated eigenfunctions are in good qualitative agreement with experimental measurements. The TAEFL calculations find frequency evolution that resembles experimental fishhook behavior; see Fig. 6 of Ref. 54. As shown in Fig. 9, the computed eigenfunction is very similar on either side of the frequency minimum, as observed experimentally.

It should be noted that the frequency downsweeps observed in JET[8,22,23] are of much longer duration than the fishhook downsweeps observed in DIII-D. Thus, it is possible that the JET modes are different.

IV. CONCLUSION

As in other tokamaks, downsweeping RSAEs are extremely rare in beam-heated DIII-D discharges. The eigenfunction and plasma conditions of downsweeping cases are similar to those of ordinary RSAEs, suggesting that they are the same mode with different stability properties. The hypothesis that downsweeping RSAEs are infernal modes is inconsistent with the data but other explanations are not excluded. The predictions of a gyrofluid model are in good agreement with the observations.

In future work, it would be interesting to use other codes to study the conditions for existence of unstable RSAEs and to compare the predicted eigenfunctions with experiment.

ACKNOWLEDGMENTS

This work was supported by the U.S. Department of Energy under SC-G903402, DE-FG03-97ER54415, DE-AC05-0000R22725, DE-AC02-09CH11466, and DE-FC02-04ER54698. We thank the DIII-D Team for their support and E. M. Bass, B. Breizman, W. Deng, and E. J. Strait for helpful discussions.

[1]Y. Kusama, H. Kimura, T. Ozeki, M. Saigusa, G. J. Kramer, T. Oikawa, S. Moriyama, M. Nemoto, T. Fujita, K. Tobita, G. Y. Fu, R. Nazikian, and C. Z. Cheng, Nucl. Fusion **38**, 1215 (1998).
[2]S. E. Sharapov, D. Testa, B. Alper, D. N. Borba, A. Fasoli, N. C. Hawkes, R. F. Heeter, M. Mantsinen, and M. G. Von Hellermann, "Contributors to the EFDA-JET Work-programme," Phys. Lett. A **289**, 127 (2001).
[3]S. E. Sharapov, B. Alper, H. L. Berk, D. N. Borba, B. N. Breizman, C. D. Challis, A. Fasoli, N. C. Hawkes, T. C. Hender, J. Mailloux, S. D. Pinches, and D. Testa, Phys. Plasmas **9**, 2027 (2002).
[4]M. A. Van Zeeland, W. W. Heidbrink, R. Nazikian, W. M. Solomon, M. E. Austin, H. L. Berk, N. N. Gorelenkov, C. T. Holcomb, A. W. Hyatt, G. J. Kramer, J. Lohr, M. A. Makowski, G. R. McKee, C. C. Petty, S. E. Sharapov, and T. L. Rhodes, Plasma Phys. Controlled Fusion **50**, 035009 (2008).
[5]M. Garcia-Muñoz, N. Hicks, R. Van Voornveld, I. G. J. Classen, R. Bilato, V. Bobkov, M. Brambilla, M. Bruedgam, H.-U. Fahrbach, V. Igochine, S. Jaemsae, M. Maraschek, K. Sassenberg, and ASDEX Upgrade Team, Nucl. Fusion **50**, 084004 (2010).
[6]D. C. Pace, R. K. Fisher, M. Garcia-Muñoz, W. W. Heidbrink, and M. A. Van Zeeland, Plasma Phys. Controlled Fusion **53**, 062001 (2011).
[7]X. Chen, M. E. Austin, R. K. Fisher, W. W. Heidbrink, G. J. Kramer, R. Nazikian, D. C. Pace, C. C. Petty, and M. A. Van Zeeland, Phys. Rev. Lett. **110**, 065004 (2013).
[8]B. N. Breizman, M. S. Pekker, and S. E. Sharapov, Phys. Plasmas **12**, 112506 (2005).
[9]H. Kimura, Y. Kusama, M. Saigusa, G. J. Kramer, K. Tobita, M. Nemoto, T. Kondoh, T. Nishitani, O. Da Costa, T. Ozeki, T. Oikawa, S. Moriyama, A. Morioka, G. Y. Fu, C. Z. Cheng, and V. I. Afanasév, Nucl. Fusion **38**, 1303 (1998).
[10]J. A. Snipes, A. Fasoli, P. Bonoli, S. Migliuolo, M. Porkolab, J. E. Rice, Y. Takase, and S. M. Wolfe, Plasma Phys. Controlled Fusion **42**, 381 (2000).
[11]R. Nazikian, G. J. Kramer, C. Z. Cheng, N. N. Gorelenkov, H. L. Berk, and S. E. Sharapov, Phys. Rev. Lett. **91**, 125003 (2003).
[12]M. Takechi, A. Fukuyama, M. Ishikawa, C. Z. Cheng, K. Shinohara, T. Ozeki, Y. Kusama, S. Takeji, T. Fujita, T. Oikawa, T. Suzuki, N. Oyama, A. Morioka, N. N. Gorelenkov, G. J. Kramer, and R. Nazikian, Phys. Plasmas **12**, 082509 (2005).
[13]M. A. Van Zeeland, G. J. Kramer, M. E. Austin, R. L. Boivin, W. W. Heidbrink, M. A. Makowski, G. R. McKee, R. Nazikian, W. M. Solomon, and G. Wang, Phys. Rev. Lett. **97**, 135001 (2006).
[14]S. E. Sharapov, B. Alper, Yu. F. Baranov, H. L. Berk, D. Borba, C. Boswell, B. N. Breizman, C. D. Challis, M. de Baar, E. De La Luna, E. A. Evangelidis, S. Hacquin, N. C. Hawkes, V. G. Kiptily, S. D. Pinches, P. Sandquist, I. Voitsekhovich, N. P. Young, and JET-EFDA Contributors, Nucl. Fusion **46**, S868 (2006).
[15]S. Hacquin, B. Alper, S. Sharapov, D. Borba, C. Boswell, J. Fessey, L. Meneses, M. Walsh, and JET EFDA Contributors, Nucl. Fusion **46**, S714 (2006).
[16]S. Hacquin, S. E. Sharapov, B. Alper, C. D. Challis, A. Fonseca, E. Mazzucato, A. Meigs, L. Meneses, I. Nunes, S. D. Pinches, and JET EFDA Contributors, Plasma Phys. Controlled Fusion **49**, 1371 (2007).
[17]E. D. Fredrickson, N. A. Crocker, N. N. Gorelenkov, W. W. Heidbrink, S. Kubota, F. M. Levinton, H. Yuh, J. E. Menard, and R. E. Bell, Phys. Plasmas **14**, 102510 (2007).

[18]M. P. Gryaznevich, S. E. Sharapov, M. Lilley, S. D. Pinches, A. R. Field, D. Howell, D. Keeling, R. Martin, H. Meyer, H. Smith, R. Vann, P. Denner, E. Verwichte, and MAST Team, Nucl. Fuson **48**, 084003 (2008).
[19]N. A. Crocker, E. D. Fredrickson, N. N. Gorelenkov, G. J. Kramer, D. S. Darrow, W. W. Heidbrink, S. Kubota, F. M. Levinton, H. Yuh, J. E. Menard, B. P. LeBlanc, and R. E. Bell, Phys. Plasmas **15**, 102502 (2008).
[20]E. M. Edlund, M. Porkolab, G. J. Kramer, L. Lin, Y. Lin, and S. J. Wukitch, Phys. Rev. Lett. **102**, 165003 (2009).
[21]E. M. Edlund, M. Porkolab, G. J. Kramer, L. Lin, Y. Lin, N. Tsujii, and S. J. Wukitch, Plasma Phys. Controlled Fusion **52**, 115003 (2010).
[22]G. J. Kramer, R. Nazikian, B. Alper, M. de Baar, H. L. Berk, G.-Y. Fu, N. N. Gorelenkov, G. McKee, S. D. Pinches, T. L. Rhodes, S. E. Sharapov, W. M. Solomon, M. A. Van Zeeland, and JET EFDA Contributors, Phys. Plasmas **13**, 056104 (2006).
[23]I. G. Abel, B. N. Breizman, S. E. Sharapov, and JET-EFDA Contributors, Phys. Plasmas **16**, 102506 (2009).
[24]M. A. Van Zeeland, W. W. Heidbrink, R. Nazikian, M. E. Austin, C. Z. Cheng, M. S. Chu, N. N. Gorelenkov, C. T. Holcomb, A. W. Hyatt, G. J. Kramer, J. Lohr, G. R. McKee, C. C. Petty, R. Prater, W. M. Solomon, and D. A. Spong, Nucl. Fusion **49**, 065003 (2009).
[25]S. da Graca, G. D. Conway, P. Lauber, D. Curran, V. Igochine, I. Classen, M. Garcia-Muñoz, J. Stober, M. A. Van Zeeland, M. E. Manso and the ASDEX Upgrade Team, Plasma Phys. Controlled Fusion **54**, 095014 (2012).
[26]I. G. J. Classen, Ph. Lauber, D. Curran, J. E. Boom, B. J. Tobias, C. W. Domier, N. C. Luhmann, Jr., H. K. Park, M. Garcia Muñoz, B. Geiger, M. Maraschek, M. A. Van Zeeland, S. daGraca, and ASDEX Upgrade Team, Plasma Phys. Controlled Fusion **53**, 124018 (2011).
[27]B. J. Tobias, I. G. J. Classen, C. W. Domier, W. W. Heidbrink, N. C. Luhmann, Jr., R. Nazikian, H. K. Park, D. A. Spong, and M. A. Van Zeeland, Phys. Rev. Lett. **106**, 075003 (2011).
[28]D. A. Spong, E. M. Bass, W. Deng, W. W. Heidbrink, Z. Lin, B. Tobias, M. A. Van Zeeland, M. E. Austin, C. W. Domier, and N. C. Luhmann, Jr., Phys. Plasmas **19**, 082511 (2012).
[29]B. Tobias, E. M. Bass, I. G. J. Classen, C. W. Domier, B. A. Grierson, W. W. Heidbrink, N. C. Luhmann, Jr., R. Nazikian, H. K. Park, D. A. Spong, and M. A. Van Zeeland, Nucl. Fusion **52**, 103009 (2012).
[30]B. Breizman, "Fast particle interaction with waves in fusion plasmas," in *Theory of Fusion Plasmas; Joint Varenna-Lausanne International Workshop*, edited by J. W. Connor, O. Sauter, and E. Sindoni (American Institute of Physics, 2006), p. 9780.
[31]B. N. Breizman and S. E. Sharapov, Plasma Phys. Controlled Fusion **53**, 054001 (2011).
[32]S. V. Konovalov, A. B. Mikhailoskii, M. S. Shirokov, E. A. Kovalishen, and T. Ozeki, Phys. Plasmas **11**, 4531 (2004).
[33]L. Yu, G.-Y. Fu, and Z.-M. Sheng, Phys. Plasmas **16**, 072505 (2009).
[34]V. S. Marchenko and S. N. Reznik, Phys. Plasmas **18**, 040701 (2011).
[35]N. N. Gorelenkov, G. J. Kramer, and R. Nazikian, Phys. Plasmas **18**, 102503 (2011).
[36]J. W. Haverkort, Plasma Phys. Controlled Fusion **54**, 025005 (2012).
[37]L. L. Lao, H. E. St. John, R. D. Stambaugh, A. G. Kellman, and W. Pfeiffer, Nucl. Fusion **25**, 1611 (1985).
[38]B. W. Rice, D. G. Nilson, and D. Wroblewski, Rev. Sci. Instrum. **66**, 373 (1995).
[39]M. A. Van Zeeland, G. J. Kramer, R. Nazikian, H. L. Berk, T. N. Carlstrom, and W. M. Solomon, Plasma Phys. Controlled Fusion **47**, L31 (2005).
[40]M. E. Austin and J. Lohr, Rev. Sci. Instrum. **74**, 1457 (2003).
[41]B. Tobias, C. W. Domier, T. Liang, X. Kong, L. Yu, G. S. Yun, H. K. Park, I. G. J. Classen, J. E. Boom, A. J. H. Donn, T. Munsat, R. Nazikian, M. A. Van Zeeland, R. L. Boivin, and N. C. Luhmann, Jr., Rev. Sci. Instrum. **81**, 10D928 (2010).
[42]D. K. Gupta, R. J. Fonck, G. R. McKee, D. J. Schlossberg, and M. W. Shafer, Rev. Sci. Instrum. **75**, 3493 (2004).
[43]W. W. Heidbrink, M. A. Van Zeeland, M. E. Austin, E. M. Bass, K. Ghantous, N. N. Gorelenkov, B. A. Grierson, D. A. Spong, and B. J. Tobias, "The effect of the fast-ion profile on Alfvén eigenmode stability," Nucl. Fusion (in press).
[44]M. A. Van Zeeland, M. E. Austin, N. N. Gorelenkov, W. W. Heidbrink, G. J. Kramer, M. A. Makowski, G. R. McKee, R. Nazikian, E. Ruskov, and A. D. Turnbull, Phys. Plasmas **14**, 056102 (2007).
[45]T. N. Carlstrom, G. L. Campbell, J. C. DeBoo, R. Evanko, J. Evans, C. M. Greenfield, J. Haskovec, C. L. Hsieh, E. McKee, R. T. Snider, R. Stockdale, P. K. Trost, and M. P. Thomas, Rev. Sci. Instrum. **63**, 4901 (1992).
[46]P. Gohil, K. H. Burrell, R. J. Groebner, and R. P. Seraydarian, Rev. Sci. Instrum. **61**, 2949 (1990).
[47]Y. Luo, W. W. Heidbrink, K. H. Burrell, D. H. Kaplan, and P. Gohil, Rev. Sci. Instrum. **78**, 033505 (2007).
[48]C. M. Muscatello, W. W. Heidbrink, D. Taussig, and K. H. Burrell, Rev. Sci. Instrum. **81**, 10D316 (2010).
[49]B. A. Grierson, K. H. Burrell, C. Chrystal, R. J. Groebner, D. H. Kaplan, W. W. Heidbrink, J. M. Muñoz Burgos, N. A. Pablant, W. M. Solomon, and M. A. Van Zeeland, Rev. Sci. Instrum. **83**, 10D529 (2012).
[50]R. Nazikian, G. Y. Fu, M. E. Austin, H. L. Berk, R. V. Budny, N. N. Gorelenkov, W. W. Heidbrink, C. T. Holcomb, G. J. Kramer, G. R. McKee, M. A. Makowski, W. M. Solomon, M. Shafer, E. J. Strait, and M. A. Van Zeeland, Phys. Rev. Lett. **101**, 185001 (2008).
[51]W. Deng, Z. Lin, I. Holod, Z. Wang, Y. Xio, and H. Zhang, Nucl. Fusion **52**, 043006 (2012).
[52]E. M. Bass and R. E. Waltz, Phys. Plasmas **20**, 012508 (2013).
[53]Y. Chen, T. Munsat, S. E. Parker, W. W. Heidbrink, M. A. Van Zeeland, B. J. Tobias, and C. W. Domier, Phys. Plasmas **20**, 012109 (2013).
[54]D. A. Spong, Nucl. Fusion **53**, 053008 (2013).